



Attorney's Docket No. 1033806-000010

IN THE UNITED STATES PATENT AND TRADEMARK OFFICE

In re Patent Application of)	MAIL STOP SEQUENCE
Snyder J. Snyder et al.)	Group Art Unit: 2877
Application No.: 10/672,889)	Examiner: HWA S. LEE
Filed: September 26, 2003)	Confirmation No.: 9565
For: METHOD AND APPARATUS FOR)	
DETERMINING THE WAVELENGTH)	
OF AN INPUT LIGHT BEAM)	

**DECLARATION UNDER 37 C.F.R. § 1.132 AS TO THE OBJECTIVE EVIDENCE
OF NONOBVIOUSNESS**

Commissioner for Patents
P.O. Box 1450
Alexandria, VA 22313-1450

Sir:

I, James J. Snyder, one of the inventors of the above-identified subject application declares as follows:

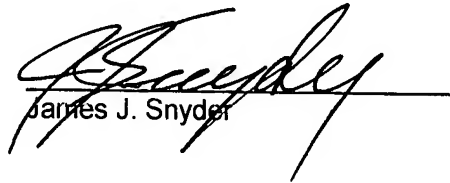
1. James J. Snyder and Stephen L. Kwiatkowski, who are inventors of the above-identified application, are the authors of a technical paper (hereinafter, paper) that is entitled "Wavelength measurement with a Young's interferometer," submitted to, peer reviewed, and published in Optical Engineering, 44 (8), 083602 (August 2005). (Exhibit A attached.)
2. The inventions described in Claims 1, 24, 35, and 44 were fully disclosed in the paper.
3. As evidenced by an article of SPIE Professional, October 2006 issue (Exhibit B attached), the paper was recognized for its innovative advancement of existing wavelength measurement technologies and selected by the Kingslake Award Committee who awarded the 2005 Rudolf Kingslake Medal and Prize to Mr. Kwiatkowski and me, the authors of the paper.

4. I hereby declare that all statements made herein of my own knowledge are true and that all statements were made on information and belief and are believed to be true; and further that these statements were made with the knowledge that willful false statements and the like so made are punishable by fine or imprisonment, or both, under Section 1001 of Title 18 of the United States Code and that such willful false statements may jeopardize the validity of the application or any patent issued thereon.

Date:

3/16/07

By:


James J. Snyder



Wavelength measurement with a Young's interferometer

James J. Snyder*
Stephen L. Kwiatkowski†
Soquel Technology, Inc.
1088 Carole Court
Matthews, North Carolina 28104

Abstract. We describe a simple, static, fiber optic laser wavelength meter based on a Young's interferometer. In this wavelength meter, the two sources are provided by unequal-length output fibers from a single-mode 3-dB directional coupler. The cleaved ends of the output fibers are held rigidly at a fixed separation facing a linear sensor array that records the sinusoidally varying fringe pattern. Analysis of the recorded fringe pattern resolves the free-spectral-range ambiguity of the interferometer and provides a high-resolution value for the wavelength of the source. Based on our investigation, we believe that with occasional recalibration, the wavelength meter is capable of an accuracy better than one part in 10^5 . © 2005 Society of Photo-Optical Instrumentation Engineers.
[DOI: 10.1117/1.2030947]

Subject terms: wavelength metrology; wavelength meters; fiber optics; telecom; instruments.

Paper 040862R received Nov. 17, 2004; revised manuscript received Feb. 21, 2005; accepted for publication Feb. 22, 2005; published online Aug. 23, 2005.

1 Introduction

A wavelength meter directly measures the absolute wavelength of light emitted by a laser.¹ Since first developed in the early 1970s, wavelength meters have been commonly used in spectroscopic studies to monitor a tunable laser as it excites some atomic or molecular transition. More recently, wavelength meters also are being used to measure the wavelength of telecom laser sources in wavelength-division multiplexed (WDM) networks to ensure that the source is properly tuned to its channel in the International Telecommunication Union (ITU) grid.

The accuracy required of a wavelength meter depends on the application. Linear spectroscopy and telecom applications typically require absolute accuracy near 10^{-6} , while nonlinear spectroscopy may require a more demanding 10^{-7} to 10^{-8} . The accuracy of commercially available wavelength meters ranges from a few parts in 10^5 to a few parts in 10^7 .

With few exceptions, wavelength meters are based on interferometry. The most common class of wavelength meter is a form of Michelson interferometer in which the incident laser beam under test is divided by a beamsplitter, sent down two different paths to moving retroreflectors that impart a smoothly varying optical path difference, and then recombined by the beamsplitter to form fringes. The fringe intensity, which oscillates as the optical path difference changes, is detected, and the oscillations are counted over some predetermined time interval. A reference laser beam,

of precisely known wavelength, is injected into the same interferometer in parallel with the laser beam under test, and the oscillations of the reference laser's fringes are counted over the same interval. The ratio of the two fringe counts is equal to the inverse ratio of the wavelengths, and since one wavelength is known, the second wavelength is easily calculated.

Michelson wavelength meters are conceptually simple, straightforward to construct, and capable of high accuracy. However, they require a reference laser as well as a translation stage to move the retroreflectors over relatively long distances at constant velocity, and are therefore not very compact or robust and do not provide very rapid updates. In addition, since they must count every fringe during a scan distance of the order of a centimeter, they are applicable only to cw lasers.

Snyder^{2,3} described a wavelength meter based on the Fizeau interferometer. This interferometer consists of a pair of glass plates, separated by a few millimeters of vacuum and oriented with a slight wedge between them. When this vacuum wedge is illuminated by a collimated laser beam the first and second surfaces of the wedge reflect beams that propagate in slightly different directions. Interference between the two beams produces a pattern of straight, uniformly spaced, sinusoidal fringes over their overlap region. Snyder showed that this fringe pattern, if recorded by a linear photodiode array and digitized, could be analyzed to determine the wavelength of the laser beam. Unlike the Michelson wavelength meters, the Fizeau wavelength meter is calibrated during manufacture, and does not require a reference laser. Because the photodiode array records the instantaneous fringe pattern, both cw and pulsed lasers can be measured. Moreover, since it has no moving parts, the Fizeau wavelength meter is inherently more robust and can provide a higher measurement update rate.

Although the Fizeau wavelength meter offers advan-

*Current address: University of North Carolina at Charlotte, Center for Precision Metrology, 9201 University City Blvd., Charlotte, North Carolina 28223; E-mail: jjsnyder@uncc.edu

†Current address: Lockheed Martin Space Systems Company, Advanced Technology Center, 3251 Hanover Street-O/ABDS B/201, Palo Alto, California 94304-1191; E-mail: Stephen.L.Kwiatkowski@lmco.com

0091-3286/2005/\$22.00 © 2005 SPIE

tages over the Michelson wavelength meter, it requires highly stable optomechanical alignment, and for applications requiring better than 10^{-6} accuracy, it was found to suffer from systematic errors related to chromatic and other aberrations and from thermomechanical instability. Some of these problems were addressed by Kachanov,^{4,5} who simplified the optical system by eliminating the collimating mirror and replacing the vacuum wedge with a glass plate with parallel surfaces. The Kachanov design produces a fringe pattern similar to the Fizeau, which can be analyzed in the same way. Although the Kachanov design is optically somewhat simpler than the Snyder design, the stability requirements are similar and in practice the performance is not improved.⁶ In addition, it proved technically difficult to reduce the package size of either the Fizeau wavelength meter or the Kachanov wavelength meter much below the size of other wavelength meters of comparable accuracy.

We are developing a fiberoptic wavelength meter based on Young's interferometer. The interferometer is formed by the cleaved ends of two single-mode optical fibers that are the output ports of a 1×2 , 3-dB directional fiber coupler. (An alternative approach would be to use a planar waveguide 1×2 , 3-dB directional coupler.) The laser radiation is coupled into the input fiber of the coupler, where it is split into roughly equal powers and radiates from the ends of the two output fibers. The lengths of the two output fibers are unequal, to provide an optical path difference. The ends of the output fibers are held parallel at a fixed separation, and with the faces flush. As in a Young's interferometer, the two output fibers emit diverging spherical waves that overlap. In the region where the wavefronts overlap, they interfere to produce straight, parallel fringes with a sinusoidal intensity profile. These fringes are similar to, and can be recorded and analyzed in the same way as the fringes of the Fizeau wavelength meter already described. Moreover, like the Fizeau wavelength meter it is calibrated during manufacture and does not require a reference laser.

Unlike other wavelength meters, there are no optical components between the sources (the ends of the fibers) and the sensor, which provides increased immunity to systematic errors related to optical aberrations, or to the mechanical instability of complex optical mounting structures. However, we found that mechanical instability of the output port fibers from the 3-dB splitter introduced a significant monotonic drift in our wavelength measurements. We attribute this drift to changes in the stress in the fiber or its buffer introduced during assembly, and we observed it to decay exponentially with a time constant of a week or two. Once characterized, this systematic error is very predictable, and can be easily compensated.

We also observed a diurnal modulation of the measured wavelength with an amplitude of a few parts in 10^6 , which we attribute to birefringence in the fiber. The modulation appeared to correlate with the rate of change in the ambient temperature and should, therefore, be correctable by proper control of the temperature of the interferometer.

The wavelength meter we describe here offers distinct advantages as a secondary wavelength standard. While it may not achieve the ultimate accuracy of a Michelson-based instrument, it should be substantially faster as well as more compact, robust, and economical. With these characteristics, and assuming occasional recalibration against a

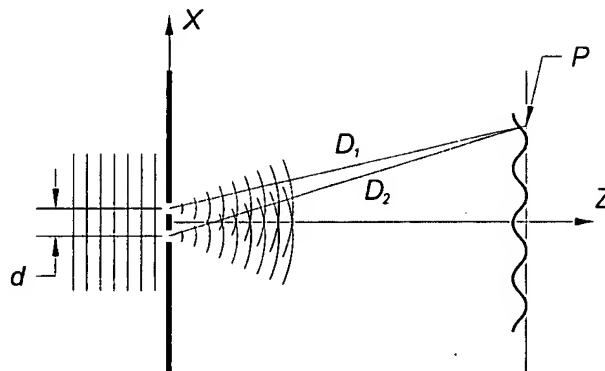


Fig. 1 Schematic showing the geometry of Young's interferometer. A plane wave incident from the left illuminates two pinholes located at $x = \pm d/2$, $z = 0$, that radiate spherical waves. Sinusoidal intensity fringes are formed at the observation plane on the right. The observation point P is located at x, z .

primary standard, it would be an obvious choice for field applications requiring wavelength measurements at remote sites.

2 Theory

The conventional form of Young's interferometer is shown in Fig. 1. The diverging spherical waves radiated from the two pinholes overlap and form sinusoidal fringes at the observation plane on the right. We define the origin of the coordinate system as a point midway between the two pinholes, which have a separation d . At an observation point $P(x, z)$ the distance from each pinhole is given by

$$D_{1,2} = \left[z^2 + \left(x \mp \frac{d}{2} \right)^2 \right]^{1/2}. \quad (1)$$

For x and $d \ll z$, the path difference from the two pinholes to the observation point is

$$D_2 - D_1 \cong \frac{xd}{z}. \quad (2)$$

In our wavelength meter we provide an offset path difference in the output fibers by cleaving them to different lengths. The optical path difference (OPD) at the observation point is then given by

$$\text{OPD} = n\Delta D_f + \frac{xd}{z}, \quad (3)$$

where ΔD_f is the path difference of the two output fibers, and n is the index of refraction of the fiber. In the observation plane at z , the fringe intensity varies sinusoidally with x ,

$$I(x) = 1 + \cos \left(\frac{2\pi n}{\lambda} \Delta D_f + \frac{2\pi xd}{\lambda z} \right), \quad (4)$$

where λ is the wavelength. (For simplicity, we ignore the difference between the wavelength in air and the wavelength in vacuum.)

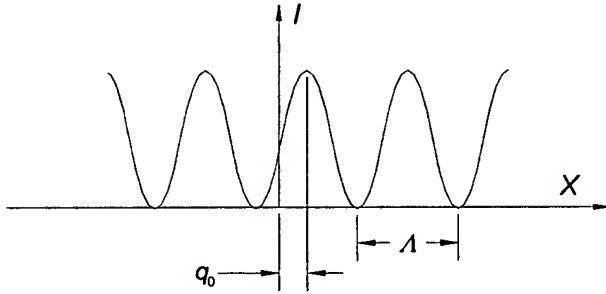


Fig. 2 Fringe intensity pattern showing the fringe period Λ and the location of the center fringe at $x=q_0$. The center of the linear photo-diode array is located at $x=0$.

The index of refraction of the fiber is approximately equal to the index of fused silica,⁷

$$n \cong \left[1 + \frac{0.6961663\lambda^2}{\lambda^2 - (0.0684043)^2} + \frac{0.4079426\lambda^2}{\lambda^2 - (0.1162414)^2} + \frac{0.8974794\lambda^2}{\lambda^2 - (9.896161)^2} \right]^{1/2}, \quad (5)$$

where λ is in units of micrometers. Although the effective index of the fiber optic core may differ slightly from the index of bulk fused silica, we assume Eq. (5) exact for purposes of calibration of the wavelength meter. Since the interferometer is sensitive only to the OPD, that assumption leads to an offset in the calibration value for the physical difference in the lengths of the output fibers. As long as the error in the index is small, the offset will not significantly affect the performance of the wavelength meter.

The variation in the index of the fiber with temperature is⁸

$$\frac{dn}{dT} = 1.1 \times 10^{-5}/\text{C}, \quad (6)$$

which implies that temperature control to ± 0.1 C would reduce temperature related errors to about $\pm 1 \times 10^{-6}$.

The fringe pattern (shown in Fig. 2) is analyzed to determine the best values (in a least squares sense) for the period of the fringes, and for $x=q_0$, the location of the peak closest to the origin. The period of the fringes, in pixels, in the observation plane is proportional to λ :

$$\Lambda(\lambda) = \frac{\lambda}{S}, \quad (7)$$

where

$$S = \frac{pd}{z} \quad (8)$$

is a scale factor, and p is the pixel pitch.

From Eq. (4), the phase at $x=0$ can be written as

$$\Phi_0 = 2\pi N, \quad (9)$$

where N , the order number of the interferometer, is inversely proportional to λ :

$$N(\lambda) = \frac{n\Delta D_f}{\lambda}. \quad (10)$$

When the wavelength meter is calibrated, lasers with known wavelengths are used to determine the scale factor S and the optical path difference of the two output fibers $n\Delta D_f$.

During each wavelength measurement, the fringe pattern is analyzed to determine the period and the position of the fringe closest to the origin, at the center of the linear array. An estimate for the wavelength λ' is found from the fringe period using Eq. (7), and the index of refraction of the fiber is calculated from Eq. (5) using the estimated wavelength. (It can be shown that the error in the index due to the use of the estimated wavelength is negligible.)

With the proper design of the interferometer, the fractional uncertainty in λ' can be much less than $1/N$. The approximate order number of interference is then

$$N' = \frac{n\Delta D_f}{\lambda'} = N + \varepsilon, \quad (11)$$

where N is the exact order number and ε is an error term such that

$$|\varepsilon| < 0.5. \quad (12)$$

The exact order number can be written as the sum of an integer and a fractional part:

$$N = N_0 + \delta N, \quad (13)$$

where the fractional part is proportional to the position of the center fringe[‡] (see Fig. 2)

$$\delta N = -\frac{q_0}{\Lambda}. \quad (14)$$

The fractional part is known accurately, since it is the result of measuring q_0 from the fringe pattern.

If we assume that the error in q_0 is negligible compared to Λ , then the error in δN can be ignored and the quantity $N' - \delta N = N_0 + \varepsilon$, rounded to the nearest integer is exactly N_0 , the integer part of the order number. The exact order number N is found from Eq. (13) and, from the exact order number, the exact vacuum wavelength is given by

$$\lambda = \frac{n\Delta D_f}{N}. \quad (15)$$

In summary, from Eq. (7), the measurement of the fringe period provides a low-resolution but unambiguous value for the order number. On the other hand, measurement of the fringe phase provides a high-resolution value for the fractional part of the order number through Eq. (14), but no information about the integer part. By combining these measurements, we can simultaneously resolve the free spectral range (FSR) ambiguity through Eq. (7), and maxi-

[‡]For simplicity, we have assumed that there is no fixed phase shift between the output arms of the coupler other than that due to the difference in the length of the arms.

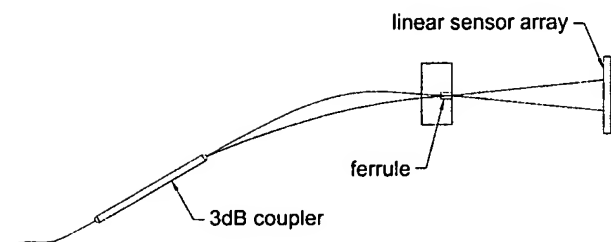


Fig. 3 Plan view of the wavelength meter. Light from the two output fibers diverges with a numerical aperture (NA) of about 0.1 and illuminates the linear sensor array located at a distance of 59.8 mm.

mize the resolution of the order number measurement through Eq. (14). The wavelength is then found through Eq. (15).

3 Wavelength Meter Description

We designed a prototype wavelength meter to operate at telecom wavelengths in the region of 1550 nm. In the plan view of the wavelength meter shown in Fig. 3, a laser is coupled into the input fiber of a 3-dB 1×2 coupler (part number 50-10335-50-21201, available from Gould Electronics, Inc., Millersville, Maryland). The coupler splits the light into equal intensities in the two output fibers, which are approximately 100 mm long and differ in length by approximately 3.1 mm. The ends of the output fibers are mounted flush and parallel in a two-hole ferrule with a separation $d=0.250$ mm.

From Eq. (5), the approximate index in the fiber at 1550 nm is 1.444, so the order number is about 2900. The FSR:

$$\text{FSR} = \frac{\lambda}{N}, \quad (16)$$

is 0.53 nm. If the error in our estimated wavelength from Eq. (7) is small compared to the FSR, it follows that the error in the approximate order number is small compared to 1, and that the approximate order number can be reduced to the exact order number.

The ends of the output fibers face an uncooled linear InGaAs sensor array (Model SUV512LD, available from Sensors Unlimited, Princeton, New Jersey) centered on the x axis at a distance of $z=59.8$ mm. The beams emitted from the two output fibers diverge with an NA of about 0.1, and form 12-mm diam overlapping spots at the array. The pixel pitch of the array is $p=0.025$ mm.

For the prototype interferometer, from Eq. (8) the scale factor is $S=104.5$ nm/pixel. From Eq. (7), the fringe period at 1550 nm wavelength is $\Lambda=14.9$ pixel at the sensor face. The pitch of the sensor pixels is $25 \mu\text{m}$, so the fringe period in micrometers is 372. We estimate that the uncertainty in the measurement of q_0 is of the order of $1 \mu\text{m}$, which justifies the assumption in the discussion following Eq. (14).

4 Fringe Processing

Typical fringe data from the sensor is shown in Fig. 4. Because the fringe positions are shifted by the slope of the envelope, the raw data is first divided by the Gaussian envelope function to reduce variations in fringe amplitude.

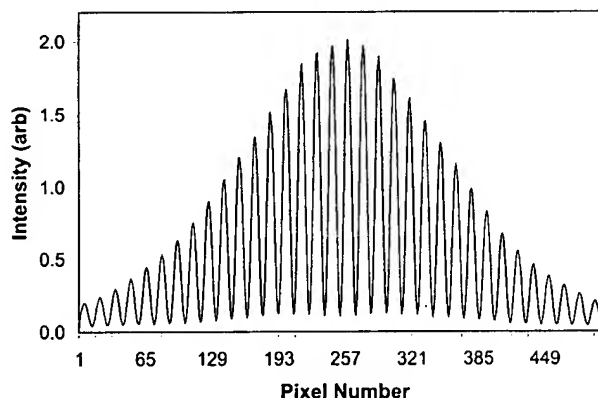


Fig. 4 Fringe intensity pattern recorded by a 512-pixel linear array with a width of 12.8 mm. The fringe period is 14.88 pixels and the $1/e^2$ width of the Gaussian envelope is 480 pixels.

The fringe spacing is then linearized by the application of weak quadratic and cubic terms that correct for the approximation of Eq. (2) and for any offset of the sensor from the z -axis. These correction terms are found empirically during the calibration process.

Next, the modified fringe pattern is digitally analyzed to find the average fringe period, Λ , and the position, q_0 , of the fringe peak nearest the center of the array.⁹ These measurement values are combined with the known calibration values S and ΔD_f and the index of refraction for the fiber, from Eqs. (5) and (6), to give the vacuum wavelength.

For the prototype wavelength meter, we collect and analyze the data using a LabView program on a personal computer. With this program, and with an integration time of 5 ms for the sensor, we are able to measure the wavelength at a 10-Hz rate. With a high-speed sensor and customized digital signal processing (DSP) electronics, the update rate should exceed 1 kHz.

5 Calibration

Initial calibration of the wavelength meter consists of finding values for the period and for q_0 at each of several different known wavelengths. This is easily accomplished using a stable, tunable laser and a higher accuracy wavelength meter. The scale factor is calculated from Eq. (7) for each calibration wavelength, and the average scale factor is stored as the calibration value. For the prototype wavelength meter, calibrated at 11 evenly spaced wavelengths from 1525 to 1575 nm, the average scale factor is $S=104.569$ nm/pixel with a standard deviation of 0.007 (7×10^{-5}). This implies an error in the approximate order number calculation of $\varepsilon \approx \pm 0.2$, which satisfies the requirement of Eq. (12).

Calibrating the difference in the length of the output fibers ΔD_f is somewhat more complex, but easy to implement. The procedure is based on comparing the measured fractional part of the order number δN from Eq. (14) with the fractional part of the calculated order number from Eq. (10). For the correct value of $n\Delta D_f$, and in the absence of noise and dispersion,

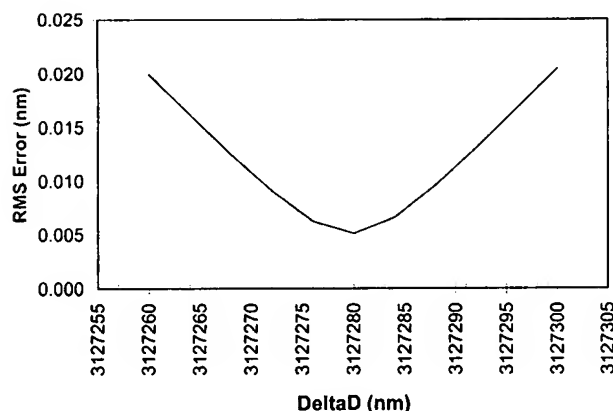


Fig. 5 The rms difference between the measured and calculated values for the fractional part of the order number as a function of the path difference ΔD_f .

$$\delta N \equiv \frac{q_0}{\lambda} = \text{Frac}\left(\frac{n\Delta D_f}{\lambda}\right), \quad \forall \lambda. \quad (17)$$

In the general case, the fractional parts will match over a wide range of wavelengths only for values of ΔD_f near the correct value. The procedure we follow is to choose a test range of values for ΔD_f that is large enough to include the correct value. For each of the test values of ΔD_f we find the root-mean-square (rms) error between the measured and calculated fractional parts over all the test wavelengths. The rms error as a function of ΔD_f drops to near zero in the immediate vicinity of the correct value, as shown in Fig. 5. This gives a calibration value for the length difference of the prototype wavelength meter of $\Delta D_f = 3.127280$ mm. The residual errors in the calculated wavelengths, based on the calibration values, are shown in Fig. 6. Over the tested wavelength range, the worst-case error was about 4×10^{-6} .

Since the most critical calibration value ΔD_f depends on the physical parameters of the fiber, it may drift with time, necessitating periodic recalibration of the interferometer. As long as the accumulated drift is small compared with the FSR, only a single reference-wavelength source is required. In most cases, recalibration consists of incrementally ad-

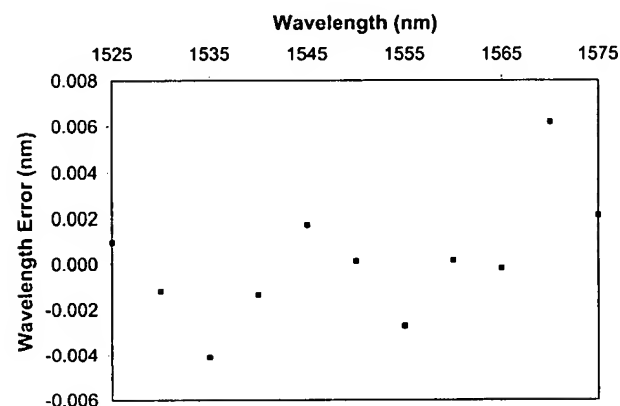


Fig. 6 Plot of the residuals between the calculated wavelength and the wavelength as measured by the commercial wavelength meter.

justing the calibration value ΔD_f by the amount necessary for Eq. (15) to yield the correct value for the wavelength.

6 Temperature Correction

Both the index of refraction of the fiber and the path difference are affected by the ambient temperature. The uncorrected change in measured wavelength with temperature at 1550 nm is

$$\frac{\partial \lambda}{\partial T} = -\lambda \left(\frac{1}{n_f} \frac{dn_f}{dT} + \alpha \right) = -0.013 \text{ nm/}^\circ\text{C}, \quad (18)$$

where $\alpha = 5.5 \times 10^{-7}/^\circ\text{C}$ is the coefficient of thermal expansion (for simplicity, we again ignore the difference between the wavelength in air and the wavelength in vacuum), and the index dependence on temperature is given in Eq. (6). To compensate temperature effects to the level of a part in 10^6 , the temperature is measured to 0.1°C , and the appropriate corrections are applied to the index calculation and the path difference. Over the typical diurnal temperature range of our laboratory, 20 to 23°C , the measured temperature coefficient from a least squares fit of several days of data uncorrected for temperature is $-0.014 \text{ nm/}^\circ\text{C}$, in reasonable agreement with Eq. (18).

For stability tests with the prototype wavelength meter, we have chosen to apply the temperature correction of $-0.014 \text{ nm/}^\circ\text{C}$ directly to the calculated wavelength, using Eq. (18), rather than applying separate corrections to n_f and ΔD_f .

7 Birefringence

Birefringence in the output arms of the splitter introduces a polarization dependence in the optical path difference of the interferometer, leading to polarization-dependent wavelength shifts. These errors are a problem for this wavelength meter because the polarization state of the input light being measured cannot be controlled in general. Moreover, in the prototype wavelength meter we observe a continuous, slow (over minutes) modulation of the measured wavelength, which we attribute to (possibly temperature-dependent) rotation of the plane of polarization of the light passing through the coupler, even when polarization-preserving fiber is used to connect the laser to the input fiber of the coupler. For the prototype wavelength meter we observe a polarization-dependent wavelength shift of $\pm 0.005 \text{ nm}$ at 1550 nm.

Birefringence in single-mode fibers is partly intrinsic, due to manufacturing defects such as core ellipticity, and partly extrinsic, due to bending or compressing of the fiber. For typical telecom fiber, such as SMF-28 (available from Corning Optical Fiber, Corning, New York), core ellipticity is $\leq 1\%$, causing an estimated¹⁰ maximum intrinsic birefringence at 1550 nm of $\beta_i \approx 0.6 \text{ rad/m}$, where β is related to the difference between the ordinary and extraordinary indices by

$$\beta = \frac{2\pi}{\lambda} (n_e - n_o). \quad (19)$$

Twisting and annealing has been shown to significantly reduce the intrinsic birefringence of fiber,¹⁰ and compressing the fiber to introduce compensating birefringence has been

demonstrated,¹¹ although we have not investigated these options.

Since the orientations of the intrinsic birefringence axes of the two output arms of the interferometer are arbitrary, the net differential retardance is estimated at ≤ 0.06 rad for the 100-mm length of the output fibers. A retardance of 0.06 rad would cause a polarization-dependent wavelength error at 1550 nm of ± 0.005 nm in the prototype wavelength meter.

Bending a fiber such as SMF-28 of radius r around a curve of radius R causes extrinsic birefringence at 1550 nm of¹²

$$\beta_e = -5.3 \times 10^5 \frac{r^2}{R^2} \text{ rad/m}, \quad (20)$$

where the minus sign indicates that the fast axis is in the plane of the curve. In the configuration of our prototype interferometer, we estimate the radius of curvature of the long and short arms of the interferometer as 250 and 125 mm, and from Eq. (20) the estimated birefringences are 0.03 and 0.13 rad/m, respectively. Since the two fibers are in the same plane, the differential birefringence of the two is 0.10 rad/m, which leads to an additional polarization-dependent wavelength shift of ± 0.001 nm.

The extrinsic birefringence of the interferometer is oriented in the plane in which the fibers are curved, whereas the orientation of the intrinsic birefringence is arbitrary. Therefore the net polarization-dependent wavelength shift could vary between ± 0.001 and ± 0.006 nm. This is consistent with our measured value of ± 0.005 nm.

8 Results

For testing purposes we connected the wavelength meter to a fixed-wavelength laser (Model MPS-8033, available from ILX Lightwave, Bozeman Montana), at a nominal wavelength of 1550 nm, monitored (through a fiber directional coupler) by a commercial wavelength meter with a specified accuracy of ± 0.003 nm (Model 86120C, available from Agilent, Englewood, Colorado). During a typical test run, with a duration of several days, the commercial wavelength meter reported a wavelength of 1553.286 nm with a drift of 0.002 nm for the laser. The temperature of the prototype wavelength meter was monitored during the tests, and the measured wavelength was corrected according to Eq. (18).

Although the prototype wavelength meter has resolution substantially better than 10^{-6} , there are two unresolved problem areas that affect the accuracy. The first problem is the sensitivity of the fibers to mechanical forces. During assembly, the fibers are positioned on the interferometer base and epoxied in place. After curing the epoxy overnight, we typically observe an initial rapid increase in measured wavelength over a period of a few days, followed by a slower, positive drift rate with a time constant of a week or two. We attribute the drift to changes in the stress within the fiber, or in the buffer, which relax over time. We assume the wavelength drift decays according to

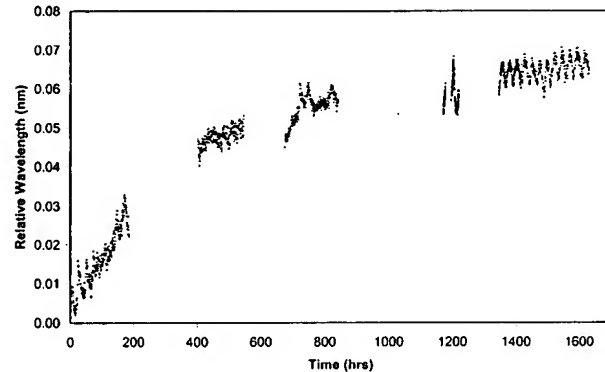


Fig. 7 Measurement data from the prototype wavelength meter intermittently monitoring a fixed-wavelength laser at 1550 nm over a 68-day period. The temperature-corrected data exhibits a decaying drift with a 15-day time constant. Most of the noise and modulation in the data is believed to be the result of fiber birefringence coupled with changes in polarization due to temperature drift.

$$\Delta\lambda(t) = A \left[1 - \exp\left(-\frac{t}{\tau}\right) \right], \quad (21)$$

where A is the asymptotic limit, and τ is the time constant. The rate of change of the wavelength drift is

$$\frac{d\Delta\lambda(t)}{dt} = \frac{A}{\tau} \exp\left(-\frac{t}{\tau}\right). \quad (22)$$

For the prototype wavelength meter we measured a drift rate of 1.3×10^{-4} nm/h 12 days after it was assembled. The data shown in Fig. 7, taken over a 2-month period, implies a time constant of about 15 days. Equation (22) predicts that after an additional month or two the drift rate should be near 10^{-7} nm/h, or 10^{-3} nm/y. At that level, recalibration would only be necessary once per year.

Birefringence, which is the second known problem area, is believed to be the source of most of the scatter and modulation seen in Fig. 7. The modulation is diurnal, but is in quadrature phase with the temperature variation. We attribute the modulation to temperature-gradient-dependent rotation of the input polarization.

If uncorrected, birefringence introduces a relative uncertainty in the wavelength measurement of the prototype of $\pm 3 \times 10^{-6}$ (one sigma). We believe these polarization-dependent errors could be reduced by placing a polarizer in front of the sensor, or by monitoring the polarization state and applying a correction in software. Both of these approaches, which we have yet to investigate, introduce additional complexity into what is otherwise a very simple device.

An alternative solution is to construct the interferometer from a custom coupler having twisted, annealed fiber with low birefringence.¹⁰

9 Conclusions

We described a very simple, compact, fiber optic laser wavelength meter based on a Young's interferometer. A prototype of the wavelength meter has been built and tested, and has demonstrated short-term accuracy, after calibration,

better than one part in 10^5 . Long-term accuracy is affected by exponentially decaying drift [Eq. (22)], as shown in Fig. 7, which we believe is predictable and could be readily compensated. The prototype interferometer is fabricated from a commercial 1×2 3-dB fiber coupler with the output arms cut to different lengths to provide an interferometric order number between 2000 and 3000. Light from the two output arms overlaps on a linear sensor array and forms sinusoidal fringes. The fringes are captured by the array and analyzed by a personal computer to determine the wavelength of the light launched into the coupler.

The accuracy of the prototype wavelength meter is adversely affected by birefringence and by drift in the optical path difference of the interferometer. The birefringence leads to a polarization-dependent uncertainty in the measured wavelength of $\pm 3 \times 10^{-6}$. The monotonic path-difference drift initially caused the measured wavelength to change at the rate of 4×10^{-5} nm/h, and appears to be decaying with a time constant of 15 days. Assuming that the drift is due to stress relaxation, the rate is expected to be below 10^{-3} nm/y within a few months after assembly.

Acknowledgments

The authors are pleased to express their gratitude to Sensors Unlimited for the loan of the InGaAs Line Camera.

References

1. J. J. Snyder and T. W. Haensch, "Laser wavelength meters," in *Topics in Applied Physics, Dye Lasers*, 3rd ed., F. P. Schaefer, Ed., pp. 201–219, Springer-Verlag, Berlin (1990).
2. J. J. Snyder, "Fizeau wavelength meter," in *Laser Spectroscopy III*, J. L. Hall and J. L. Carlsten, Eds., pp. 419–420, Springer-Verlag, Berlin (1977).
3. J. J. Snyder, "Apparatus and method for determination of wavelength," U.S. Patent No. 4,173,442 (Nov. 1979).
4. A. A. Kachanov, "Interferometer with processor for linearizing fringes for determining the wavelength of laser light," U.S. Patent No. 5,420,687 (May 30, 1995).
5. A. A. Kachanov, "Interferometer with alignment assembly and with processor for linearizing fringes for determining the wavelength of laser light," U.S. Patent No. 5,543,916 (Aug. 6, 1996).
6. *New Focus Model 7711 Users' Manual*, New Focus, Inc., Santa Clara, CA (2002).
7. M. Thomas and T. J. Harris, "Properties of crystals and glasses," Chap. 33 in *Handbook of Optics*, Vol. II, M. Bass, Ed., p. 33.69, McGraw-Hill, New York (1978).
8. E. J. Friebele, M. A. Putnam, H. J. Patrick, A. D. Kersey, A. S. Greenblatt, G. P. Ruthven, M. H. Krim, and K. S. Gottschalk, "Ultra-high-sensitivity fiber-optic strain and temperature sensor," *Opt. Lett.* **23**, 222–224 (1998).
9. J. J. Snyder, "Algorithm for fast digital analysis of interference fringes," *Appl. Opt.* **19**, 1223–1225 (1980).
10. A. H. Rose, Z. B. Ren, and G. W. Day, "Twisting and annealing optical fiber for current sensors," *J. Lightwave Technol.* **14**, 2492–2498 (1996).
11. C. A. Villarruel, M. Abebe, and W. K. Burns, "Birefringence correction for single-mode fiber couplers," *Opt. Lett.* **7**, 626–628 (1982).
12. R. Ulrich, S. C. Rashleigh, and W. Eickhoff, "Bending-induced birefringence in single-mode fibers," *Opt. Lett.* **5**, 273–275 (1980).



James J. Snyder is a research professor with the Center for Precision Metrology, Department of Mechanical Engineering and Department of Physics and Optics, the University of North Carolina at Charlotte. He received his PhD degree in electrical engineering from the State University of New York at Stony Brook in 1973, and has been with NIST (formerly NBS), Lockheed, and the Lawrence Livermore National Laboratory (LLNL). He founded or cofounded three companies: Blue Sky Research, Soquel Technology, and Fizeau Electro-Optic Systems. Dr. Snyder holds more than two dozen patents and has published numerous scientific papers. His current research interests include laser beam propagation codes, precision optical measurement of sphere radii, and laser wavelength meters.



Stephen L. Kwiatkowski earned his BS degree from the University of Michigan, Dearborn, in 1979, his MS degree from the Institute of Optics, the University of Rochester, in 1985, and his PhD degree from the University of Colorado in 1995. He is currently with Lockheed Martin's Advanced Technology Center in Palo Alto, California. His research interests include guided-wave devices and their applications to metrology.

MEMBERSHIP

EXHIBIT B

In Memoriam: Dino Pongeggi



Dino Pongeggi, SPIE Fellow and past SPIE President passed away this July.

Bernard G. "Dino" Pongeggi passed away on 2 July after a battle with cancer and heart disease. Born September 1925, he was 80 years old. Growing up in New Jersey, after high school he enlisted in the Navy and saw combat in the European theater during World War II on the destroyer USS Edison. After the war he attended college at Bergen County Junior College and Brooks Institute of Photography in Santa Barbara, CA. He married his high-school sweetheart, Norma, in 1951. Pongeggi brought his family to the San Francisco Bay Area where he started work in the photo technology branch of the Ames Research Center in 1956. Shortly thereafter, Ames Research Center became part of the National Aeronautics and Space Administration (NASA).

During his 32 years with NASA, Pongeggi

worked on a variety of important programs including the Viking and Pioneer programs, the Earth Resource Aircraft Project (ERAP), the Mercury, Gemini, and Apollo programs as well as early space shuttle work.

While working at NASA, Pongeggi became active with SPIE. He held numerous local and national positions in SPIE, including president (1970-1972). He was made a Fellow of the Society in 1977, and received the SPIE President's Award in 1982.

"SPIE has lost a very good friend," says Sue Davis, SPIE director of special projects, who worked with Pongeggi during his years of activity with the Society. "He truly was one in a million, and I personally will miss his infectious smile and generous soul."

Snyder, Kwiatkowski Receive Kingslake Medal and Prize



James J. Snyder



Stephen L. Kwiatkowski

The 2005 Rudolf Kingslake Medal and Prize has been awarded to James J. Snyder and Stephen L. Kwiatkowski for their paper "Wavelength measurement with a Young's interferometer," published in the August 2005 issue of *Optical Engineering*. Selected by the Kingslake Award Committee, this paper is recognized for its innovative advancement of existing wavelength measurement technologies.

In the award-winning paper, the authors describe a fiber-optic laser wavelength meter based on a Young's interferometer. The wavelength meter described is similar to those based on Michelson and Fizeau interferometers, but simpler and more robust, thus making it ideal for field applications that require wavelength measurements from remote locations. In addition, the meter is more compact in size, requiring no reference laser, and is substantially faster than other wavelength meters. Based on their analysis, the authors conclude that with occasional recalibration, the wavelength meter is capable of accuracy better than one part in 10^5 .

Snyder is a research professor with the Center for Precision Metrology, Department of Mechanical Engineering and Department of Physics and Optics, at the University of North

Carolina at Charlotte. He founded/co-founded Blue Sky Research, Soquel Technology, and Fizeau Electro-Optic Systems, and holds more than two dozen patents. His current research interests include laser beam propagation codes, precision optical measurement, and laser wavelength meters.

Kwiatkowski is at Lockheed Martin's Advanced Technology Center in Palo Alto, CA. His accomplishments include five patents and co-founding Soquel Technology. Kwiatkowski's research interests include guided-wave devices and their applications to metrology.

The Rudolf Kingslake Medal and Prize is presented annually in recognition of the most noteworthy original paper to appear during the previous year in the SPIE journal *Optical Engineering*, on the theoretical or experimental aspects of optical engineering. Award winners receive a citation and honorarium of \$2,000.

Read the award-winning paper online at spie.org. In fact, if you've chosen the journal *Optical Engineering* as part of your membership package, you can read the paper free of charge.